Brain Stimulation 19 (2026) 102981

Contents lists available at ScienceDirect

Brain Stimulation

journal homepage: www.journals.elsevier.com/brain-stimulation

Non-invasive temporal interference stimulation of the hippocampus suppresses epileptic biomarkers in patients with Epilepsy: biophysical differences between kilohertz and amplitude modulated stimulation

Florian Missey [a,b,1], Emma Acerbo [c,d,1], Adam S. Dickey [d], Jan Trajlinek [a], Ondřej Studnička [a], Claudia Lubrano [a], Mariane de Araújo e Silva [a], Evan Brady [d], Vit Všianský [e], Johanna Szabo [f], Irena Dolezalova [e], Daniel Fabo [f], Martin Pail [e], Claire-Anne Gutekunst [c], Rosanna Migliore [g], Michele Migliore [g,h], Stanislas Lagarde [b,i], Romain Carron [b,j], Fariba Karimi [k], Raul Castillo Astorga [m], Antonino M. Cassara [k], Niels Kuster [k,l], Esra Neufeld [k], Fabrice Bartolomei [b,i], Nigel P. Pedersen [m], Robert E. Gross [c,n], Viktor Jirsa [b], Daniel L. Drane [d,o,p], Milan Brázdil [e], Adam Williamson [a,q,*]

[a] International Clinical Research Center, St. Anne's University Hospital Brno, 60200, Brno, Czech Republic
[b] Aix-Marseille Université, Inserm, Institut de Neurosciences des Systèmes (INS) UMR_S 1106, Marseille, France
[c] Department of Neurosurgery, Emory University School of Medicine, Atlanta, GA, USA
[d] Department of Neurology, Emory University School of Medicine, Atlanta, GA, USA
[e] Brno Epilepsy Center, 1st Department of Neurology, St. Anne's Univ. Hospital and Faculty of Medicine, Masaryk University, member of the ERN EpiCARE, 60200, Brno, Czech Republic
[f] Institute of Neurosurgery and Neurointervention, Semmelweis University, Budapest, Hungary
[g] Institute of Biophysics, National Research Council, Palermo, Italy
[h] SUNY Dept. of Neurology, Downstate Health Science University, Brooklyn, NY, USA
[i] APHM, Timone Hospital, Epileptology Department, Marseille, France
[j] Department of Functional and Stereotactic Neurosurgery, Timone University Hospital, Marseille, France
[k] Foundation for Research on Information Technologies in Society (IT'IS), Zurich, Switzerland
[l] Department of Information Technology and Electrical Engineering, Swiss Federal Institute of Technology (ETH), Zurich, Switzerland
[m] Department of Neurology, School of Medicine and Center for Neuroscience, University of California, Davis, CA, USA
[n] Department of Neurosurgery, New Jersey Medical School and Robert Wood Johnson Medical School, Rutgers University, New Jersey, USA
[o] Departments of Pediatrics, Emory University School of Medicine, Atlanta, GA, USA
[p] Department of Neurology, University of Washington School of Medicine, Seattle, WA, USA
[q] Center for Social and Affective Neuroscience, Department of Biomedical and Clinical Sciences, Linköping University, Sweden

ARTICLE INFO

Keywords:
Temporally interfering electric fields
Non-invasive brain stimulation
Neuromodulation
Epileptic biomarkers
sEEG
Amplitude modulation
Conduction block

ABSTRACT

Introduction: Medication-refractory focal epilepsy creates a significant clinical challenge, with approximately 30 % of patients deemed ineligible for surgery due to involvement of eloquent cortical regions within the epileptogenic network. For these patients, electrical neuromodulation represents a promising alternative therapy. We investigated the potential of non-invasive temporal interference (TI) electrical stimulation in reducing epileptic biomarkers in patients with mesiotemporal epilepsy (MTLE)

Material and method: Thirteen patients implanted with stereoelectroencephalography (sEEG) depth electrodes received TI stimulation with an amplitude modulation (AM) frequency of 130 Hz (Δf), delivered through either low-frequency (1 kHz + 1.13 kHz) or high-frequency (9 kHz + 9.13 kHz) carrier waves, specifically targeting the hippocampus—a common epileptic focus in MTLE. Intracerebral recordings before, during, and after TI stimulation were compared to recordings during sham stimulation at varying high-frequency (HF) carrier frequencies (1, 2, 5, and 9 kHz).

* Corresponding author.International Clinical Research Center, St. Anne's University Hospital Brno, 60200, Brno, Czech Republic.
E-mail address: adam.williamson@fnusa.cz (A. Williamson).
[1] co-first authors, contributed equally.

https://doi.org/10.1016/j.brs.2025.11.008
Received 7 June 2025; Received in revised form 8 November 2025; Accepted 8 November 2025
Available online 11 November 2025

Results: TI stimulation resulted in a statistically significant decrease in interictal epileptiform discharges (IEDs) and pathological high-frequency oscillations (HFOs), particularly fast-ripples (FR), with prominent suppression observed in the hippocampal focus and reduced propagation brain-wide. In contrast, HF sham stimulation at 1 kHz frequency partially reduced cortical IED rates without effectively reaching the hippocampal focus. This cortical impact diminished progressively at higher sham frequencies (2, 5, and 9 kHz), exhibiting depth-dependent attenuation—a phenomenon not observed with TI stimulation, irrespective of carrier frequency. Additionally, TI stimulation demonstrated a significant carry-over effect, suppressing epileptic biomarkers beyond the stimulation period, which was not evident following kHz sham stimulation.
Conclusion: Our findings underscore the therapeutic potential of TI as a non-invasive brain stimulation modality for epilepsy, offering significant suppression of epileptic biomarkers through subthreshold modulation of the epileptogenic zone. Furthermore, this study highlights distinct biophysical differences between kilohertz-frequency stimulation and focal amplitude-modulated stimulation, supporting TI's unique utility in neuromodulation research.

1. Introduction

Epilepsy presents a significant neurological challenge, as the origins of seizure generation in the brain are highly patient-specific, limiting initial treatment options to generalized medications which lack targeted precision [1]. Additionally, one-third of patients with seizures are drug-resistant, leaving resective surgery as the primary treatment option [2]. However, approximately 30 % of drug-resistant patients are not suitable candidates for resective surgery due to the high functional importance of areas necessitating resection [2]. In such cases, invasive brain stimulation – specifically deep brain stimulation (DBS) or responsive neurostimulation (RNS) – is typically the remaining therapeutic option [3]. Alternative neuromodulation treatments, such as Vagus Nerve Stimulation (VNS), are available for drug-resistant epilepsies but generally do not achieve complete seizure freedom [4–7].

Both DBS and RNS are challenging, as there are numerous potential targets (e.g., anterior nucleus of the thalamus - ANT, centromedian nucleus of the thalamus - CMT, pulvinar, hippocampus, and neocortex) [8–12], and only a small number of targets (notably the ANT, CMT and hippocampus) have been thoroughly evaluated in double-blinded studies. DBS stimulation at 130–145Hz of either the hippocampus or ANT resulted in a reduction of seizure frequency [10–14], along with a decrease in interictal epileptiform discharges (IEDs) in temporal lobe epilepsy patients [15–18]. A motivation for our study is that a subset of patients do not respond favorably to DBS or RNS and can suffer cognitive side effects, which are difficult to predict ahead of implantation [19–21].

Non-invasive brain stimulation techniques targeting these regions identified as suitable DBS or RNS locations, could support the prediction of post-implant side effects prior to invasive implantation. The most common non-invasive techniques include transcranial alternating current stimulation (tACS), transcranial direct current stimulation (tDCS), and transcranial magnetic stimulation (TMS) – techniques with applications in both research and clinical practice [22]. The methods modulate brain activity via electric currents delivered through the scalp and skull, or induced magnetically, and influence neuronal excitability, connectivity, and plasticity, ultimately leading to changes in brain function [23]. However, efficacy of traditional non-invasive methods in the treatment of epilepsy is limited, and the methods are typically considered applicable only to shallower cortical targets and not to the deep structures associated with therapeutic invasive DBS [24].

Temporal Interference (TI) stimulation is an emerging non-invasive electrical stimulation technique which allows electrical modulation of deep brain structures. Unlike traditional methods, TI applies high frequency currents (>1 kHz) using a minimum of two independent pairs of transcutaneous stimulation electrodes. The employed frequencies differ slightly, resulting in an amplitude-modulated field because of alternating phases of constructive and destructive interference. The kHz current pathways are optimized to maximally and selectively amplitude-modulate the field at a specific deep brain target where the fields overlap [25]. The amplitude modulation (AM) frequency is equal to the frequency difference ($\Delta f = |f1 - f2|$). When Δf is in the physiological range, there is evidence that neural activity is modulated. Notably, the frequency of the AM in previous experiments has been selected to match conventionally applied DBS frequencies to produce similar effects [26]. TI has been tested in rodent [27–32] and non-human primate [33] models, and more recently, in healthy human subjects [34].

We have previously employed TI stimulation using a 130 Hz envelope frequency, a frequency often used for invasive DBS in epilepsy patients and in epileptic animal models, and known to suppress epileptic biomarkers [27].

In this work, we analyzed the impact of TI with a 130Hz AM signal in patients with epilepsy. Patients implanted with stereo-electroencephalography (sEEG) depth electrodes were hospitalized for 2–3 weeks to assess potential resective surgery targets. sEEG electrodes are implanted to record intracranial electrophysiological signals and stimulate precise deep brain areas in order to assist in the delineation of the epileptogenic zone (EZ) and its relation with eloquent cortices. Utilizing recordings from the sEEG electrodes during TI, we were able to investigate alterations in epileptic biomarkers as a function of TI stimulation ($\Delta f = 130$Hz frequency modulation) and to map the applied AM signal in order to ascertain its hippocampal focality. The study has taken place at three research centers, Emory University (USA), St. Anne's University Hospital (Czech Republic), and Semmelweis University (Hungary).

Our results demonstrate that TI stimulation significantly decreases interictal epileptiform discharges (IEDs) and pathological high-frequency oscillations (HFOs) – specifically fast-ripples (FR) – within the hippocampal focus and reduces propagation across the brain. In contrast, sham stimulation at lower kilohertz (kHz) frequencies impacted cortical but not hippocampal IEDs, with diminishing effectiveness at increasing kHz frequency. Furthermore, a therapeutic short term carry-over effect – the suppression of epileptic biomarkers for a period of time after the end of stimulation – was only observed for AM and not for unmodulated kHz. The results suggest distinct differences in biophysical mechanisms and associated response characteristics from kHz compared to focal AM.

2. Methods

The study is registered as a clinical trial with clinicaltrials.gov (NCT06716866).

Patients: 13 patients with drug-resistant focal epilepsy and a clinical diagnosis of medial temporal epilepsy participated in the study after providing informed consent (see Table 1). All procedures involving human participants were conducted following the ethical standards of the institutional and/or national research committee (IRB00099109 Emory University, IIT/2023/25 Saint-Anne University Hospital - SAUH, OGYÉI/56526-2/2023 Institute of Neurosurgery and Neurointervention, Semmelweis University - INN-SU) and in accordance with

the 1964 Helsinki Declaration and its later amendments or comparable ethical standards. All participants underwent video-EEG characterization of seizures and either 1.5 or 3 T MRI, and PET scans in some patients. Presurgical non-invasive examinations, including high-resolution MRI scans, were performed to assess patient eligibility. Intracerebral multi-contact electrodes (Alcis® - INN-SU, Hungarian center; Dixi® - Emory University, USA center and SAUH, Czech center; 10–18 contacts) were surgically implanted for sEEG exploration. Postoperative computed tomography (CT) scans and/or MRI scans were conducted to verify the absence of complications and ensure accurate electrode placement using the GUI-based open-source application GARDEL [35]. Across all centers, patients underwent the stimulation protocols 6–10 days post-implantation. Patients were randomly assigned to either TI-Sham or Sham-TI sequencies for SAUH. Both patients and the analyst of the data were blinded of the stimulation group; however, due to skin sensation, two patients from EMORY university got unblinded without effect on the data which remain consistent with the group.

Power analysis: Based on sample size calculate and *a priori* – based on literature [64,65] – expectation of a large effect of our intervention (Cohen's d ~0.7), 13 patients provide 80 % power to detect a 25 % change in epileptic discharge rate between TI and baseline or post-stimulation.

Modeling and simulations: Finite element simulations were executed utilizing both Sim4Life and the Sim4Life TI Planning Tool software developed by Zurich MedTech AG to estimate temporal interference stimulation. The simulations solved the ohmic-current-dominated electro-quasistatic equation $\nabla(\sigma\nabla\phi) = 0$. Here, σ denotes the local electrical conductivity, ϕ the electric potential, and the E-field is obtained as $E = -\nabla\phi$. The ohmic-current-dominated electro-quasistatic approximation of Maxwell's equations is suitable because $\sigma \gg \omega\epsilon$ (ω: angular frequency, ϵ: permittivity, i.e., ohmic currents dominate over displacement currents) and the wavelength is much larger than the domain size.

The human model utilized in the Sim4Life simulations was derived from patient-specific MRI scans (co-registered T1 and CT). The head model for each patient included the associated implanted sEEG electrodes. All patients had the sEEG locations included in the model for postprocessing. However, only the patients from the FNUSA center had the sEEG electrodes properly modeled with recording contacts as Perfect Electrical Conductors (PEC) and inter-contacts as insulators. Tissue and electrode conductivities were automatically allocated to the model based on the ITI'S Foundation tissue properties database [36] (low--frequency conductivities section). Stimulation electrodes mirrored the shape of the gel-based electrodes used in human experiments. Simulation results were normalized to total current, after applying Dirichlet boundary conditions at active electrodes. Equation (1) from Grossman et al., 2017 [25], was used to calculate the maximum modulation amplitude:

$$\left|\overrightarrow{E}^{max}{}_{AM}(\overrightarrow{r})\right| = 2\left|\overrightarrow{E_2}(\overrightarrow{r})\right| \quad if \quad \left|\overrightarrow{E_2}(\overrightarrow{r})\right| < \left|\overrightarrow{E_1}(\overrightarrow{r})\right|\cos\alpha$$

Otherwise

$$\left|\overrightarrow{E}^{max}{}_{AM}(\overrightarrow{r})\right| = \frac{2\left|\overrightarrow{E_2}(\overrightarrow{r}) \times \left(\overrightarrow{E_1}(\overrightarrow{r}) - \overrightarrow{E_2}(\overrightarrow{r})\right)\right|}{\left(\overrightarrow{E_1}(\overrightarrow{r}) - \overrightarrow{E_2}(\overrightarrow{r})\right)}$$

Equation 1. Maximum amplitude modulation formula.

Recordings: All studies were conducted with participants in the waking state. sEEG signals were recorded digitally (1024 or 2048 Hz, Natus Medical Incorporated®, Emory), or with a BioSDA09 (25 kHz, M&I, spol. s r.o.®, INN-SU and SAUH). The latter has an input signal voltage of ± 25 mV, with an optional hardware filter of 0.01 Hz–10 kHz), which allows to monitor stimulation voltages (sEEG artifact) during TI or sham stimulation.

Stimulation (TI/sham): Stimulation was applied to target the mesial temporal lobe with the target centered on the head of the hippocampus given that most IEDs originated from the hippocampus and the hippocampal formation was part of the epileptogenic network from which seizures originated.

TI stimulation was performed using two DS5 devices (Digitimer®, UK) driven by a function generator (Keysight®). Scalp electrodes (circular-shaped gel-assisted ECG electrodes, Ag/AgCl, 0.8 cm diameter, Ambu® or FIAB®) were used for TI stimulation. They were placed according to *Violante* et al. [34] to target the hippocampus and in accord with Sim4Life modeling. Frequencies of TI stimulation varied among centers: Emory used 1300 and 1430 Hz, and the Czech and Hungarian centers 9000 and 9130 Hz, applying ±2 mA per pair (4 mA peak-to-peak). There were two protocols: In the first (SAUH and INN-SU), 20 min of baseline recording, followed by either sham stimulation (day one at SAUH and INN-SU), or active TI (day two), followed by 20 min of recording after the cessation of TI (see Fig. 2A). At Emory University, all participants underwent 20 min of baseline, 20 min of sham/active TI and 20 min of post-TI recording (day one and two), with an additional recording of 20 min on day three. In the sham condition, the same carrier frequency was applied to both channels ($\Delta f = 0$Hz, same current magnitudes as applied in the TI session), such that no amplitude modulation resulted. In the active TI condition, there was an offset frequency of 130 Hz - a typical frequency used for neuromodulation in epilepsy.

AM Analysis: Gardel was used to accurately localize sEEG electrode contacts. Briefly, the T1 MRI was co-registered with the post-implantation CT and electrodes were labeled. For the analysis of TI waveforms, the recorded signal underwent bandpass filtering (1 kHz–10 kHz). The AM magnitude was computed using the Hilbert transformation of the filtered signal. A sliding window of 230 ms was employed to determine the peak-to-peak amplitude of the AM in mV by subtracting the minimum from the maximum AM values. The median

Table 1
Participant characteristics. Ages are displayed in ranges of 5 years to ensure anonymization of the patients. All patients enrolled in the present study showed a temporal lobe epilepsy without clear seizure onset zone delineated at the time of the enrollment. None of the demographic factors were considered cofounding for this study.

Patient	Age	Sex	Center	Head ∅	N° of electrodes	SOZ	Day PI	Target hippocampus
P1	35–39	F	SAUH	59	8	Right temporal lobe	6	Right
P2	40–44	M	SAUH	61	13	Left Insular lobe	6	Left
P3	35–39	M	SAUH	60	11	Left temporal lobe	6	Left
P4	45–49	F	SAUH	60	8	Bi-temporal lobes	6	Left
P5	40–44	M	SAUH	61	8	Left temporal lobe	6	Left
P6	35–39	M	EMORY	54	10	Bi temporal lobe	7	Left
P7	25–29	M	EMORY	60	13	Left parietal lobe	7	Left
P8	35–39	M	EMORY	58	18	Left temporal lobe	7	Left
P9	30–34	F	INN-SU	58	8	Left temporal lobe	8	Left
P10	40–44	M	INN-SU	61	6	Left temporal lobe	7	Left
P11	45–49	F	INN-SU	60	7	Right temporal lobe	6	Right
P12	25–29	M	SAUH	61	12	Right temporal lobe	6	Right
P13	30–34	F	SAUH	60	14	Left temporal lobe	6	Left

value across all windows was utilized as the amplitude value for each contact. This process was conducted for each contact, providing amplitude values per contact (the reference was set as the averaged signal from all the electrodes in the brain). Finally, the amplitude values were projected onto the electrodes within the anatomical mesh of the patient to visually assess which brain regions received stimulation (Fig. 1C).

Biomarkers Detection: For the detection of biomarkers, electrophysiological signals were filtered (lowpass filtering [<1000Hz], performed using Matlab - MathWorks) to remove the stimulation artifacts. After down-sampling to 2500 Hz, semi-automatic detection of IEDs and HFOs (ripples and fast ripples) was performed using the AnyWave's validated Delphos detector [37] – a well-established IED and HFO detector, regularly used in clinical epilepsy research [38]. Events markers (IEDs, HFOs) were extracted to determine their rates per minute. Subsequently, detected events were manually validated using AnyWave, a visualization software for electrophysiological data [37].

Statistics: The results of the detection process were imported into MATLAB (MathWorks), to facilitate comprehensive analysis and statistical assessment, and organized into distinct matrices based on patient

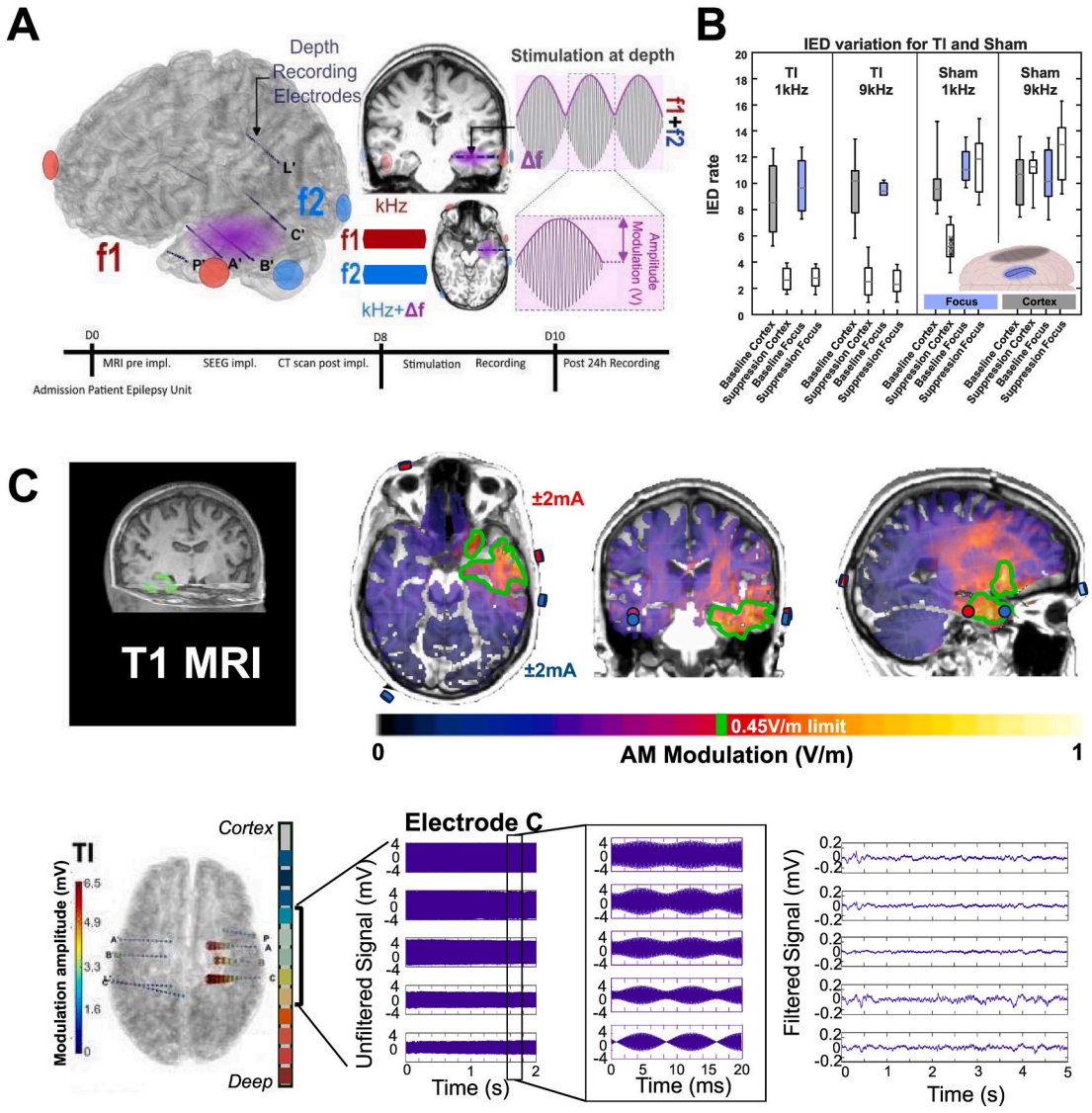

Fig. 1. Temporal interference protocol in sEEG-implanted patients with epilepsy. (**A**) Scalp electrodes were positioned to deliver TI stimulation, consisting of two high-frequency currents which produce an AM field targeting the hippocampus in the temporal lobe. sEEG electrodes simultaneously record the electrophysiological signal and the modulated TI stimulation signal. Timeline of the experiments performed at the three centers: Admission Day 0, Stimulation Days 8–9. Each center applied TI with an AM frequency $\Delta f = 130$Hz, during a 20-min stimulation session and recorded the brain signal response before, during, and after stimulation. **(B)** The effect of TI stimulation does not seem to depend on carrier frequency with TI delivered by low and high carriers suppressing activity. However, sham stimulation effect is highly dependent on frequency – with 1 kHz applied on the scalp having some inhibitory effect only on cortical regions and 9 kHz having no effect overall; see Figs. 2 and 3. (**C**) **Patient-specific head model and AM signal from TI stimulation.** MRIs of patients were used to create patient-specific head models using Sim4Life. (Top panel) the example simulation shows the placement of stimulation electrodes (red/blue) to target the ipsilateral hippocampus. The green border depicts an isocontour of the AM electric field, indicating the highest region of modulation centered on the hippocampus. (Bottom panel) simulations compare well to intracranial data, which similarly shows maximum AM in the temporal lobe (electrodes A, B, C, and Supplemental Fig. S6), specifically in the hippocampus. Example recordings from the middle contacts of electrode C are shown. The raw signal (with using the average of all intracranial signals as reference) during TI stimulation allows visualization of the amplitude of the AM signal. When zooming in, the stimulation artifact revealed a well-defined AM in the deepest contacts, with diminishing magnitude approaching the cortex. The exact same recordings during TI stimulation are shown filtered with a bandpass filter ([1–1000] Hz) to extract electrophysiological signals. All oscillations below 500Hz were recovered, and reduced interictal spiking activity was observed for the TI condition.

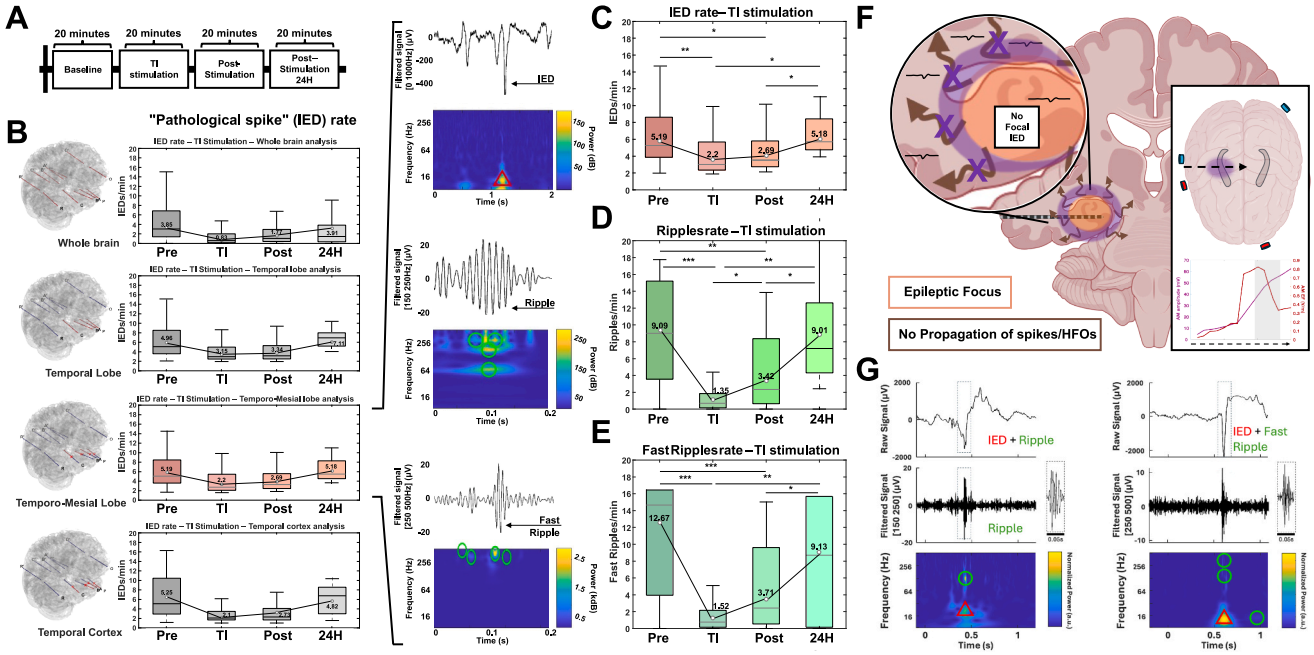

Fig. 2. Epileptic biomarkers are suppressed during TI stimulation, and a post-stimulation carry-over effect is observed. (**A**) The stimulation protocol was the same across the different centers (USA, Czech Republic, Hungary). Center-to-center differences are shown in Supplemental Fig. S1. The protocol includes baseline recording (20 min), TI stimulation protocol (20 min; 30-s ramp-up and 30-s ramp-down included), post-stimulation recording (20 min), and – only in Czech Republic – post-24-h recording (20 min). (**B**) Analysis of IEDs rates by brain region. All regions show a decrease in IED rate during TI stimulation. Analysis comparing all biomarker rates across all centers from the mesial temporal focus (n.s: p-value >0.05; *: p-value ≤0.05; **: p-value ≤0.01; ***: p-value ≤0.001). (**C**, **D**, and **E**) Looking at the epileptic focus in detail: TI stimulation significantly decreases IEDs, ripples, and FRs, in a way similar to responses in DBS studies [40,41]. A feature of the TI biomarker suppression is that, in addition to the suppression during stimulation, the biomarkers do not return to their pre-stimulation values in the 20-min period after stimulation – the suppression has a strong carry-over effect, consistent with other TI studies. The 24-h recordings indicate that the suppression is not permanent, seeing that biomarkers have returned to their pre-stimulation values. Brain-wide suppression of IEDs is a good indication that the focus of the epilepsy (the location of spike generation; in these patients the mesial temporal region, specifically the hippocampus) has been suppressed. (**F**) As the focus was suppressed (where the AM electric field was the more dominant), we expected and observe limited generation and therefore limited propagation of IEDs and HFOs. For full size image of the AM potential/EF, see Fig. S6. (**G**) The simultaneous suppression of HFOs and IEDs is understood via co-occurrence: it is well-known that HFOs strongly co-occur within IEDs [43,44]. This co-occurrence also appears in our data.

identifiers, treatment centers (EMORY, INN-SU, or SAUH), and protocol conditions (baseline, stimulation, sham, post, and post 24H). From these matrices, initial visualizations were generated for each patient before aggregation for inter/intra-patient and inter/intra-center statistical assessments. IED, ripple ([80 250]Hz), and FRs ([250 500]Hz) rates were computed and juxtaposed across different stimulation protocols, as illustrated in Fig. 2, employing multivariate analysis of variance (ANOVA or Friedman test) and paired T or Mann-Whitney-Wilcoxon tests to discern significant variations. The aggregated dataset underwent further comparison via Friedman ANOVA and paired Wilcoxon tests to identify potential differences across all experimental conditions. All p-values presented in this manuscript are FDR corrected to minimize type I errors.

Single neuron modeling: To study the interaction between a hippocampal CA1 pyramidal neuron and electrical fields we used a previously published model [39,40], available online on the ModelDB database (a.n. 151731 and 190559, respectively). A detailed morphological and biophysical reconstruction of a CA1 pyramidal neuron [41] (cellc62564 from Migliore et al. (2008), ModelDB a.n. 87535) was used for all simulations. A first set of simulations was performed in current clamp mode, injecting one or two currents for 1 s and implemented as Equation (2) at different amplitudes I_0.

$$I_{inj} = I_0\ sin\ \ sin\ [2\pi f(t-t_0)] \text{ or } I_{inj} = I_0\ sin\ \ sin\ [2\pi f(t-t_0)] + I_0\ sin\ \ sin\ \left[2\pi\left(f+f_{off}\right)(t-t_0)+\varphi\right]\Big)$$

Equation 2. Injected current formula.

All simulations were performed using v.8.2.2 of the NEURON simulation environment (Hines and Carnevale, 1997) [42].

3. Results

3.1. Temporal interference protocol in sEEG-implanted epilepsy patients

TI stimulation was performed in patients with drug-resistant mesial temporal lobe epilepsy implanted with sEEG electrodes (Fig. 1A). Epilepsy patients with implanted sEEG electrodes offer a unique opportunity to precisely delineate the stimulated zone and assess the impact of TI exposure on brain activity. sEEG electrodes recorded the electrophysiological signal changes evoked by TI and mapped the AM exposure from the TI stimulation. The setup involved the placement of four scalp electrodes (2 pairs of 2 electrodes) to deliver TI stimulation, which consisted of two high-frequency signals unilaterally targeting the hippocampus (the side of the epileptogenic network) (Fig. 1A and C). An overview of results is seen in Fig. 1B, (left panels) TI delivered through low-frequency (1 kHz + 1.13 kHz) or high-frequency (9 kHz + 9.13 kHz) carrier waves, creating $\Delta f = 130$ kHz in the hippocampus, suppressed pathological activity in the hippocampal focus and subsequent propagation to the cortex. As further seen in Fig. 1B, (right panels) sham stimulation delivered through low-frequency (1 kHz + 1 kHz) or high-frequency (9 kHz + 9 kHz) carrier waves, creating no offset with $\Delta f = 0$ kHz, created significantly different results. Only low-frequency kHz sham reduced pathological activity, limited only to cortex and with not as pronounced a reduction as the TI. High-frequency kilohertz did not

reduce any pathological activity.

3.2. Simulation and visualization of stimulation Site

As seen in Fig. 1C (top left panel), an MRI image of a patient with stimulation electrodes specifically targeting the ipsilateral hippocampus is seen. The associated patient-specific simulation of the TI exposure (top right panels) targeting the hippocampus is visualized using Sim4life software. The simulation estimates the electrode position for a correct stimulation of the hippocampus and delineates the region of strong AM modulation (green border) within the temporal region - with the maximum modulation located in the patient's hippocampus.

3.3. Recordings of AM potential

An example sEEG recording of the AM potential during TI stimulation can be seen in Fig. 1C (bottom panels). The amplitude of the AM was extracted and is depicted on the contacts of each sEEG electrode in the figure. The highest AM was observed on the electrodes within the temporal lobe, specifically in the hippocampus, and showed good agreement with the patient-specific Sim4Life simulations. The AM magnitude progressively diminishes towards more superficial cortical regions, while the magnitude of the carrier increases. An analysis of the filtered signal (1–1000 Hz) demonstrated the ability to extract electrophysiological signals (IEDs/HFOs), as TI stimulation artifacts are generally several thousand Hz higher than the electrophysiological signal of interest. No IEDs are visible in the example recording.

3.4. Epileptic biomarker suppression with TI

All patients underwent baseline, stimulation, and post-stimulation recordings (see Fig. 2A) consisting of 20 min blocks: baseline recording, TI stimulation, post-stimulation recording (in the 20 min after the stimulation), and (at FNUSA only) an additional post-stimulation recording 24 h after the stimulation session. During TI stimulation, patients did not report any symptoms, such as sensations associated with TI stimulation on the scalp, or other subjective symptoms with frequencies centered at 9 kHz; 2 patients out of 3 receiving TI at 1/1.13 kHz felt tingling on the scalp without any adverse events. There were no adverse events.

We compared the distribution of IEDs detected by sEEG in various brain regions (see Fig. 2B): the whole brain (all SEEG contacts), the temporal lobe (electrodes A,B,C, and P from the most impaired side), the temporo-mesial area (deep contacts – 1 to 7 – from electrodes A,B,C, and P from the most impaired side)(the hippocampal focus), and the temporal cortex (shallow contacts – 8 to 15 – from electrodes A,B,C, and P from the most impaired side). All analyses were realized with the 'global group' encompassing all patients from the three centers. In baseline recordings, all patients showed signs of temporal lobe epilepsy, with a mesial focus. TI stimulation produced a statistically significant decrease in IEDs rate across all brain regions, which suggests that the focus was suppressed (IEDs originating from an unsuppressed additional focus would be visible). Post-stimulation data shows a strong carry-over effect with IEDs not returning immediately to baseline values. The post-stimulation recording 24 h later shows that the IED rate returned to the baseline level, the carry-over effect is not permanent.

Specific analysis of TI's impact on the epileptic biomarkers (IEDs, ripples, and FRs), specifically in the temporo-mesial region with the hippocampal focus, is presented in Fig. 2C, D, and E. All epileptic biomarkers were statistically decreased during TI stimulation in the focus compared to the baseline recordings (Friedman ANOVA, p-value <0.0001, $W = 0.66$). In all three centers, TI stimulation of the mesial temporal lobe was correlated with a decrease in IEDs (data for each participating center in supplemental figures). The relative decrease ranged up to 86.3 % (58.5 ± 27.8 %, IC95 %) depending on the patient (Friedman ANOVA, $p\text{-value}_{\text{TI stimulation vs. baseline}} < 0.0001$, $W = 0.66$).

For HFOs, it is well established that excessive pathological ripples [43] and pathological fast ripples [44] co-occur within IEDs (see Fig. 2G). Our data shows a reduction of IEDs with a corresponding reduction of co-occurring HFOs [45,46].

For all three centers, the stimulation effect was sustained, as evidenced by a significant decrease in IEDs and HFOs 20 min after stimulation (Wilcoxon tests, $p\text{-value}_{\text{Post-stimulation 20 min vs. baseline}} < 0.0001$, $r = 0.75$). TI stimulation (Fig. 2F; purple) targeting the pathological mesial focus (orange) shows a strong suppression of epileptic biomarkers, and a suppression of the propagation of biomarkers, with a short lasting sustained post-stimulation carry-over effect.

3.5. Epileptic biomarkers suppression with kHz (sham) stimulation

As TI is delivered via a combination of kHz frequencies, we investigated the effect of sham stimulation, where both pairs of electrodes provide the same frequency, and no offset is present between f1 and f2 (Fig. 3A).

As seen in Fig. 3A, all sham patients underwent the same protocol in blocks of 20 min: a baseline recording, kHz sham stimulation (two pairs of electrodes with no offset frequency – applying the same currents as for TI stimulation), and a post-stimulation recording (for 20 min after stimulation). The electrode locations were also identical to the TI stimulation electrode locations. Patient-specific Sim4Life simulations were performed to determine the carrier field magnitude distribution. The illustrative visualization in Fig. 3B delineates the region of maximum kHz exposure (top panel), situated in the temporal region, and the expected absence of AM (middle panel). sEEG electrodes were used to record the electrophysiological signal changes evoked by sham and to map the sham exposure potential (bottom panel). The example recording features IEDs in the mesial focus (highlighted by red arrow), but not in the cortex where there is a higher kHz field magnitude.

The effects of kHz sham on biomarker rates are shown in Fig. 3C, D, and E, as a function of depth along the sEEG electrode into the ipsilateral hippocampal focus. IEDs, ripples, and FRs rate changes are pictured in C, D, and E respectively. Fluctuations outside of the ±20 % range are considered a clear indication of kHz suppression of a biomarker, rather than physiological variations between the two 20-min sessions of baseline and sham [47]. Vertical dotted lines represent the depth at which the sham stimulation starts to decrease the biomarkers. For the considered electrodes, contacts #15 – #10 are located in lateral cortices and contacts #9 – #1 are in the medial cortices (including hippocampus).

Higher frequencies (i.e. 7 and 9 kHz) show less biomarker reduction compared to lower carrier frequencies (i.e. 1 and 2 kHz) in the superficial cortices. Lower frequencies are, furthermore, associated with deeper penetration of rate changes. 9 kHz sham minimally impacts these biomarkers.

As shown in detail for 1 kHz and 9 kHz in Fig. 3 F, G, and H, a common trend is visible across all biomarkers: sham-stimulation induced decreases in IEDs and HFOs (ripples and fast ripples) at lower kHz frequencies in the lateral, but not deeper medial cortices/hippocampus, and had no significant decrease at 9 kHz. Additionally, for low-frequency kHz biomarker suppression, there is no measurable carry-over effect. When comparing these SHAM results with the TI results shown above, using a multivariate ANOVA (rate ~ stimulation protocol * frequency * time), we see a global effect of stimulation protocol * frequency * time (p-value <0.05), more precisely, the value of the carrier frequency plays a role only for SHAM stimulation and the effect of the stimulation is higher during the stimulation rather than after the stimulation (for SHAM stimulation, rates before and after the stimulation are not significant (for 1 kHz). Moreover, when considering the anatomical

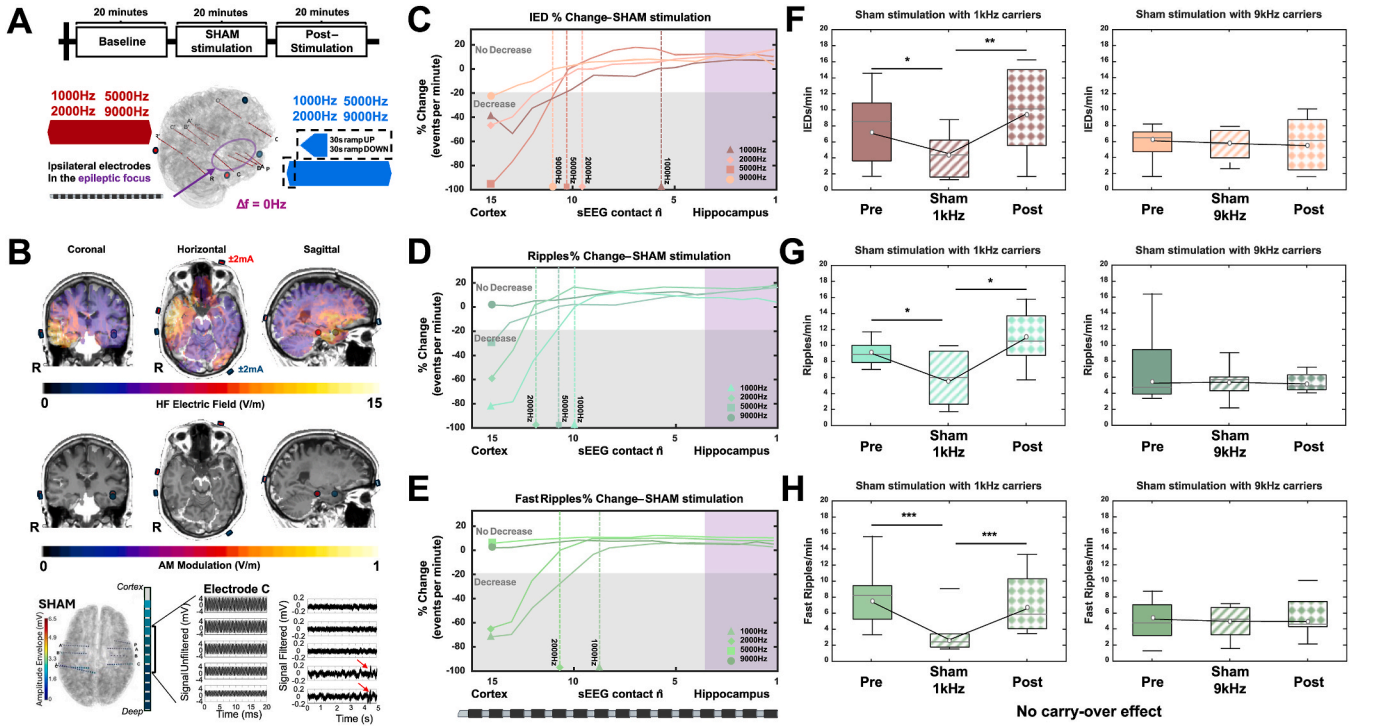

Fig. 3. Sham stimulation and IED/HFO suppression. Sham stimulation consisted of applying the same frequency ($f_1 = f_2$) to both pairs of electrodes. The protocol is 20 min baseline recording, 20 min sham stimulation and recording, and 20 min post-stimulation recording. A 30-s ramp-up and a 30-s ramp-down is included to avoid unwanted transients. The stimulation amplitude is ±2 mA (4 mA peak-to-peak) (**A**). Similar to the TI stimulation condition, a patient-specific simulation is performed to estimate the kHz field strength and illustrate the absence of AM. The sham voltage recorded by sEEG in a patient is visualized. After filtering, example IEDs (red arrows) are apparent in the hippocampus recordings, but not in the cortical recordings (**B**). The changes in biomarker rate between baseline and sham stimulation are plotted as a function of location along the ipsilateral sEEG electrode entering the pathological hippocampus. The zero line (dashed line) and grey region denote the absence of a significant rate difference between baseline and sham. sEEG contact locations in the epileptic focus are highlighted in purple. A biomarker rate reduction of over 20 % is considered a clear indication of sham suppression. As can be seen, suppression penetrates the deepest at 1 kHz, but not to the hippocampus. At 9 kHz change remains below ±20 % throughout for all biomarkers (**C**, **D**, **E**). Biomarkers are plotted for the three parts of the sham protocol using the lateral cortical contacts – sEEG contacts 15 to 8 (**F**, **G**, **H**). 1 kHz caused a significant suppression during stimulation in the cortex, potentially due to a type of subthreshold conduction block. 9 kHz did not cause significant suppression. In each case, there was no visible carry-over effect, unlike in the TI conditions.

region on the rate decrease over the different protocols (TI vs. SHAM), using a multivariate ANOVA (rate ~ stimulation protocol * frequency * region), we could highlight a region specificity of the stimulation (p-value <0.05 for the interaction). The SHAM stimulation with low-frequency carriers at 1 kHz shows a significant decrease in biomarkers only in the cortical regions when the SHAM 9 kHz does not show any decrease and when the TI (either 1 or 9 kHz) shows an overall decrease in the whole brain.

Previous studies using simulations of injected charge with a Hodgkin–Huxley (HH) axon model have suggested kHz conduction block as a possible side-effect of TI deep brain modulation [48]. Specifically, models predict that a deep brain region may respond to the AM signal, but shallower brain regions will be subjected to stronger kHz fields which may lead to conduction block. Although perhaps not "conduction block" in the traditional sense of suprathreshold stimulation of peripheral nerves, we believe that we have observed a similar phenomenon when using lower frequency kHz carriers for TI, and as predicted by the models, the phenomenon diminishes as the kHz frequencies increase further - as neural activation thresholds increase with kHz frequency (Fig. 4B). To avoid the phenomenon, one can use a higher carrier frequency. However, some models predict that shifting the carrier frequency up (while maintaining Δf constant) to reduce conduction block, will simultaneously reduce the modulatory effectiveness of AM. We do not observe this experimentally. More precisely (deep contacts – 1 to 7 – from electrodes A, B, C, and P from the most impaired side), we did not see any reduction in the effectiveness of epileptic biomarker suppression by using higher carrier frequencies when comparing the biomarker rates during TI stimulation (Wilcoxon tests, p-value$_{TI1000Hz\ vs\ TI9000Hz} > 0.05$, $r = 0.69$). Moreover, we compared TI and Sham protocols, along with timings (baseline/stimulation/post-stimulation) using a two-way repeated- ART ANOVA to assess the within protocols and identifying time-dependent effects per conditions. All TI protocols and Sham stimulation with 1 kHz significantly reduce all biomarkers rates (p-value <0.05, $\eta^2 = 0.63$); however TI protocols seem to be more efficient than 1 kHz Sham overall – refer back to Fig. 1B. In contrast, Sham 9 kHz does not induce any modulation in IED, ripples, or fast ripples rates, within the protocol or compared to TI protocols and Sham 1 kHz (p-value <0.05 when comparing Sham 9 kHz with all other protocols).

Across all analyses, effect sizes were large (0.63–0.75), consistent with our *a priori* power assumptions.

Overall, these results suggest that TI stimulation can reduce HFOs and IEDs, when targeting the hippocampus with a modulation at a traditionally inhibitory frequency (130 Hz). For sham, mid/low-carrier frequencies (≤5 kHz) also decrease the number of epileptic biomarkers, but only in superficial cortices. With a 130 Hz AM, the highest carrier frequency we tested (9 kHz) caused a significant decrease in all epileptogenic biomarkers, while the corresponding sham condition, did not change ripple and fast ripple rates, and had the least effect on IEDs. The carrier frequency selection seems to play an important role for the use of TI as a focal, non-invasive form of deep brain modulation, i.e. 9 kHz induces less off-target neuromodulation than 1 kHz, due to the absence of kHz carrier field effects.

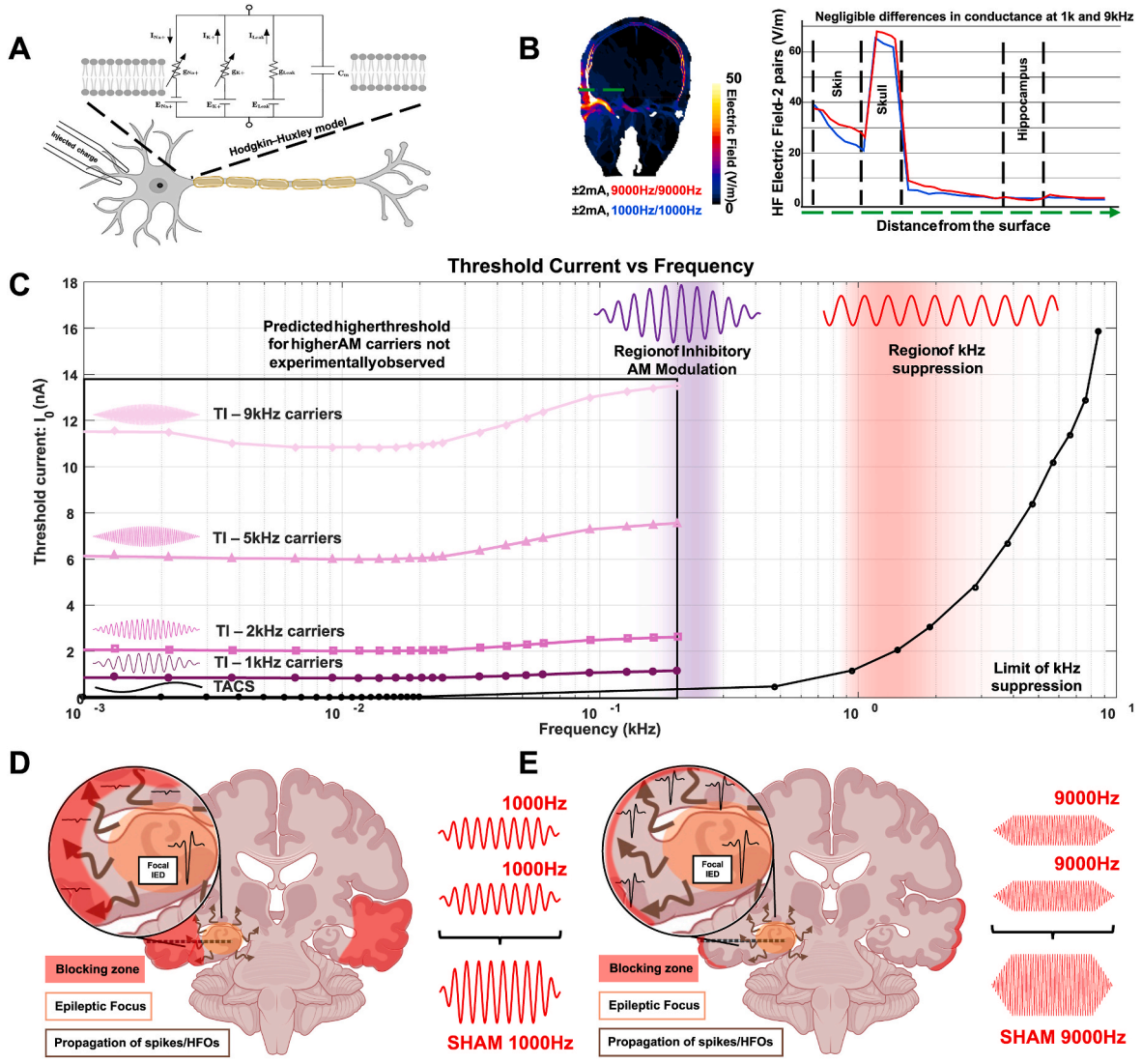

Fig. 4. Biophysics Insights. A) Previous work simulating exposure-induced suprathreshold neuromodulation of a Hodgkin–Huxley-like (HH) axon model has highlighted the potential for conduction block in TI stimulation [48]. Our sham stimulation results are consistent with some of the concerns raised by those authors. **B)** Conductivities and permittivities implemented in the simulations are based on Gabriel et al., 2009 [49]; values can be revised if new conductance measures become available. The carrier frequency dependence of sham effects cannot be explained by field magnitude differences, as electrical conductivity hardly depends on frequency below 10 kHz, such that for identical channel current magnitudes the quasistatic solutions to Maxwell equations are very similar – only at much higher frequencies does the frequency dependence of conductivity and its impact on displacement currents become relevant. Also head and contact impedance changes as a function of frequency are fully compensated for by the current control of the sources (see Supplemental Fig. S5). **C)** Experimental work by Bernard Katz [50] and simulations with an HH-like neuron model, showed that the threshold for propagation blocking by unmodulated exposure (red shading) increases with frequency (the threshold obviously depends on diameter, fiber type, etc). This is in accordance with the kHz suppression (where we use the word suppression and not block, as we apply subthreshold electric fields) of IED propagation from the mesial focus observed in this study for low kHz sham frequencies and the experimentally demonstrated decrease in the suppression depth with increasing carrier frequency (fading red). However, the HH model fails to replicate the experimentally observed absence of a strong carrier frequency impact on AM effectivity. Moving to a higher carrier frequency eliminated sham effects - however, the AM signal created with the same higher carrier frequency suppressed the epileptic focus without apparent reduction in efficacy (purple region). **(D–E).** Support for assuming that two different mechanisms are at work could be derived from the lack of a carry-over effect from sham stimulation (turning off the high frequency allowed activity to propagate normally again), while AM exposure produced a strong carry-over effect, where suppression of the hippocampal focus resulted in a continued reduction of epileptic biomarkers post-stimulation.

4. Discussion

Here we show for the first time that a non-invasive deep brain modulation method, Temporal Interference, can selectively target the epileptic focus and reduce epileptiform activity in epilepsy patients, as verified by intracerebral EEG recordings. We show that TI can create an AM signal at depth in the human mesial temporal lobe and that TI stimulation at $\Delta f = 130$Hz can significantly reduce IEDs, ripples, and FRs during stimulation.

Furthermore, we show that the choice of carrier frequencies matters for neuromodulation with TI. As simulated in Fig. 4A and C, our results are partly consistent with previous simulated work using the HH model to suggest that unmodulated kHz carrier signals could modulate brain activity, experimentally verified by us via the presence of biomarker suppression, primarily in superficial cortical structures at low kHz frequencies (red region). However, suppression mechanisms explained by high-frequency conduction block, as well as simple HH models of neural dynamics, fail to explain the observed carry-over effects produced by

AM signals and fail to explain how TI with higher kHz carriers produces targeted, non-invasive, deep brain modulation, with no penalty in terms of effectiveness compared to TI with lower kHz carriers – something which previous studies had ruled out based on theoretical and computational considerations [51]. As predicted by Hodgkin-Huxley (HH) models— AM and kHz fields are strongly attenuated requiring significantly higher currents (e.g., X mA more at 9 kHz versus 2 kHz) to elicit comparable modulation effects – however we did not experimentally observe this (purple region). AM with 9 kHz carriers modulated pathological brain activity equally well as AM with 1 kHz carriers, however 9 kHz had significantly reduced sham effects. This highlights the importance of clarifying the mechanisms underlying TI neuromodulation.

Clearly electrical brain modulation is not governed only by the amplitude of an applied electrical signal, as the performance of kHz and AM is dramatically different in the suppression of pathological brain activity. The human brain is a complex interconnected network of cells: astrocytes, oligodendrocytes, microglia, ependymal cells, endothelial cells/pericytes, and finally neurons which are further subdivided into excitatory vs inhibitory cells. These interconnected networks form large circuits and subcircuits, which naturally generate their own inherent electrical brain rhythms. It is entirely reasonable to assume, and as we have experimentally demonstrated, that such a system could be more sensitive to some electrical waveforms and more invariant to other externally applied electrical waveforms.

Finally, and often an important point overlooked in simplified in vitro and modelling studies, TI modulation of the human brain applies *subthreshold* electric fields, with the AM electric field typically no more than a few V/m. This subthreshold AM electric field has a spatial extent across a volume of width equal to many SEEG contacts (Fig. 1C; Fig. S6), where the AM signal volume is superimposed over the underlying brain network of similar volume and tissue inhomogeneity, interacting with the various cell types in the region, the specific interconnected networks, and the natural rhythms entering, exiting, and generated by the target region. We therefore find it unsurprising that AM delivered via TI and unmodulated kHz signals yield different results.

In terms of future utilization in epilepsy, the application of TI stimulation represents a significant advancement in the pursuit of non-invasive diagnosis and therapy for epilepsy, particularly for patients who are not suitable candidates for resective surgery. Unlike conventional transcranial electrical stimulation techniques, such as tDCS and tACS, which are limited by the dominance of superficial cortical effects, TI stimulation allows for the modulation of neural activity in deeper brain structures without invasive procedures. This is particularly relevant for targeting epileptogenic zones located in areas of the brain which are not easily accessible by traditional stimulation methods or only by electrical stimulation via depth probes [52,53]. While our patient-specific modeling and sEEG-recorded AM amplitudes demonstrate focality centered on the hippocampus (Fig. 6) – as focal as possible with only two pairs of stimulation electrodes, it is acknowledged that adjacent mesial temporal structures may experience co-stimulation due to the spatial spread of the electric fields. We recently adapted standard TI protocols to increase their spatial focality by integrating more pairs of stimulation electrodes which could better delineate the stimulation minimize off-target impacts while maximizing therapeutic specificity [33]. This type of more complex stimulation protocol could be easily used in subsequent studies to assess the level of necessary focality to get a therapeutical effect of TI stimulation in patients with epilepsy.

In previous work, TI stimulation in the peripheral [29] and central nervous systems modulates population-wide neural activity [54] as well as individual neuronal activity [55], when employing Δf frequencies similar to those found to be effective when applied directly (i.e. $\Delta f =$ 1Hz modulating activity at a rate of 1 Hz – as is expected if 1Hz is directly applied). Indeed the DARPA project in the United States investigating TI has recently shown sleep enhancement using a 1 Hz envelope frequency to increase slow-wave sleep (a brain state associated with approximately 1 Hz natural brain rhythms), with high-frequency carriers of 15 kHz, and with no sham effects when testing the unmodulated kHz alone [66]. Our findings here are similarly in line with previous research, namely studies conducted in the hippocampus of mice in an epilepsy model [27] as well as with various clinical studies which have used DBS stimulation (130–145Hz) in the hippocampus of patients to manage their seizures and decrease epileptogenic biomarkers [3,10,13,14,56–58].

The choice of 130 Hz as the amplitude modulation frequency in this study was informed by its widespread use in invasive neuromodulation for epilepsy, including responsive neurostimulation devices like NeuroPace (typically 100–200 Hz, most commonly 130 Hz), which reduce cortical excitability and seizure frequency. These parameters were originally adapted from DBS for movement disorders, and while ideal settings for epilepsy remain an active research area, we prioritized those with the strongest evidentiary support for efficacy. Personalizing the frequency based on individual patient biomarkers, such as IED patterns or seizure dynamics, could optimize outcomes and merits exploration in future trials. Furthermore, theoretical modeling using finite element simulations indicated electric field enhancements around the implanted sEEG electrodes, attributable to their high conductivity relative to surrounding brain tissues (Fig. S7). Even if present in the simulations, this field enhancement is negligeable as the size of the relevant enhancement remains extremely small compared to the tissue damages induced by the electrode implantation. Additionally, Lamos and colleagues [59] further show no physical measurements of such field enhancement around implanted electrodes although present in the simulations.

While the cohort of 13 patients across three centers provides preliminary evidence of TI's effects on epileptic biomarkers, this sample size is relatively small for drawing robust statistical conclusions, particularly when subdivided by carrier frequency groups (low vs. high kHz). These differences could introduce confounding factors; however, aggregated data analyses revealed consistent biomarker suppression patterns across centers (Figs. S1–S3), bolstered by large effect sizes (Cohen's $d \approx 0.7$). Moreover, although the observed suppression of IEDs and HFOs in this study is interpreted as indicative of therapeutic potential, supported by correlations in DBS literature where such biomarker reductions are associated with improved seizure control, we recognize that no direct data on seizure frequency or clinical outcomes were collected during these acute sessions. This constitutes a limitation of the current work, as biomarker changes alone do not conclusively demonstrate anti-seizure efficacy. To address these limitations of the study, an ongoing long-term study is ongoing to investigate the effects of repeated TI stimulation over a large group of patients and with different stimulation sessions to evaluate impacts on seizure burden and patient-reported outcomes.

5. Conclusion

The application of TI stimulation in patients with epilepsy represents a novel and promising approach in the non-invasive treatment of epilepsy. TI stimulation at $\Delta f = 130$ Hz non-invasively suppresses hippocampal epileptic biomarkers in patients with mesial temporal lobe epilepsy, with short-term carry-over after stimulation and reduced superficial off-target effects when using higher carrier frequencies without reduction of modulatory effect. The utilization of 130 Hz aligns with previous invasive neuromodulation literature and preclinical TI studies while indicating mechanistic differences between unmodulated kHz carriers and amplitude-modulated fields.

As a final thought, additional future work could leverage TI for cognition in epilepsy, specifically the ability of TI to reduce IEDs non-invasively and in a targeted manner, as there is growing awareness that IEDs transiently disrupt focal and global cognitive processes and

anti-seizure medications are currently not deliverable in a focal manner [60–63]. In that sense, TI could be a valuable tool in neurological investigation of cognitive task performance with epilepsy patients. Indeed, even for conduction block, as we observed for lower kHz frequencies, it is possible that this mechanism could be used beneficially in the context of epilepsy in future work.

While our preliminary findings are encouraging, further research is essential to elucidate the potential of TI stimulation to manage other focal epilepsies, not exclusively MTLE, and perhaps as a tool to assess neurostimulation responses prior to DBS or RNS implantation. Future research will need to expand the number and diversity of studied patients undergoing TI stimulation across different types of epilepsies and perhaps assess the long-term impact of stimulation – for example possible strategies to extend the length of the observed carry-over effect to increase the period of time with suppressed epileptic activity. Indeed, increasing the number of available options for therapy can only benefit patients suffering from drug-resistant epilepsy.

CRediT authorship contribution statement

Florian Missey: Writing – review & editing, Writing – original draft, Visualization, Formal analysis, Data curation, Conceptualization. **Emma Acerbo:** Formal analysis, Data curation. **Adam S. Dickey:** Methodology. **Jan Trajlinek:** Methodology, Formal analysis, Data curation. **Ondřej Studnička:** Methodology, Formal analysis, Data curation. **Claudia Lubrano:** Methodology, Investigation. **Mariane de Araújo e Silva:** Methodology, Investigation. **Evan Brady:** Investigation. **Vit Všianský:** Investigation. **Johanna Szabo:** Investigation. **Irena Dolezalova:** Investigation. **Daniel Fabo:** Investigation. **Martin Pail:** Investigation. **Claire-Anne Gutekunst:** Investigation. **Rosanna Migliore:** Formal analysis. **Michele Migliore:** Formal analysis. **Stanislas Lagarde:** Investigation. **Romain Carron:** Investigation. **Fariba Karimi:** Formal analysis. **Raul Castillo Astorga:** Investigation. **Antonino M. Cassara:** Formal analysis. **Niels Kuster:** Formal analysis. **Esra Neufeld:** Formal analysis. **Fabrice Bartolomei:** Investigation. **Nigel P. Pedersen:** Writing – review & editing, Writing – original draft, Formal analysis, Conceptualization. **Robert E. Gross:** Investigation. **Viktor Jirsa:** Formal analysis. **Daniel L. Drane:** Writing – review & editing, Writing – original draft, Formal analysis, Conceptualization. **Milan Brázdil:** Investigation, Conceptualization. **Adam Williamson:** Writing – review & editing, Writing – original draft, Methodology, Conceptualization.

Authors Contribution

A.W. conceived and designed the project. F.M., E.A., A.D., J.T., O.S., C.L., M.A.S., E.B., V.V., J.S., D.F., conducted human experiments and acquired neural data. F.M. and E.A. analyzed neural data. F.M. created the patient-specific head models and performed the associated finite-element models. R.M. and M.M. designed and analyzed single-neuron models. F.K. and E.N. investigated the implant related field enhancement. F.M., E.A., D.L.D., and A.W. wrote the first draft of the manuscript and refined it after inputs from I.D., M.P., C.A.G., S.L., R.C., F.K., R.C.A., A.M.C., N.K., E.N., F.B., N.P.P, R.E.G, V.J., and M.B.

Data Availability Statement

Access to data is subject request to the corresponding authors, to research ethics committee approval and completion of a data sharing agreement.

Declaration of competing interest

The authors declare no competing financial or personal interests related to this study. Niels Kuster and Esra Neufeld are shareholders of TI Solutions AG, a company dedicated to producing Temporal Interference (TI) stimulation devices. However, the TI Solutions AG commercial TI stimulator was not used in this study, which employed independently assembled research equipment. All other authors declare no conflicts of interest.

Acknowledgments

A.W. received funding from the European Union#8217; s Horizon Europe research and innovation programme under grant agreement No. 101101040 (TREATMENT) and No. 101088623 (EMUNITI). Efforts on this project for both D.L.D. and E.A. were in part supported by grants received from the National institute of Neurological Disorders and Stroke (NINDS) of the National Institutes of Health (NIH) [R01NS088748]. E.A. was also supported through the Emory Neuromodulation Technology Innovation Center (ENTICe) and a Catalyst Award from the Emory Neurosurgery Department to C.A.G. and D.L.D. E.A. was also supported by the American Epilepsy Society (AES) postdoctoral fellowship. We thank S. Dabiri for his assistance in downloading MRI and electrophysiological recordings. We extend our thanks to the dedicated nurses at the epilepsy units of Emory University, St. Anne's University Hospital, and Semmelweis University for their invaluable support. This work received financial support from Agence Nationale de la Recherche under France 2030 bearing the reference "ANR-24-RRII-0005 », on funds administered by Inserm. This work was also supported by the Ministry of Health of the Czech Republic in cooperation with the Czech Health Research Council in the context of the RECOVERY project under No. NW25J-04-00094 (F.M.). We acknowledge a contribution from the Italian National Recovery and Resilience Plan (NRRP), funded by the European Union – NextGenerationEU (Project IR0000011, CUP B51E22000150006, 'EBRAINS-Italy', and Project PRIN 2022ZY5RXB_002 'HIPPOCOMP'), and the EU Horizon Europe Programme under the Specific Grant Agreement No. 101147319 (EBRAINS 2.0 Project).

Appendix A. Supplementary data

Supplementary data to this article can be found online at https://doi.org/10.1016/j.brs.2025.11.008.

References

[1] Fiest KM, Sauro KM, Wiebe S, et al. Prevalence and incidence of epilepsy: a systematic review and meta-analysis of international studies. Neurology 2017;88(3):296–303. https://doi.org/10.1212/WNL.0000000000003509.
[2] Ryvlin P, Cross JH, Rheims S. Epilepsy surgery in children and adults. Lancet Neurol 2014;13(11):1114–26. https://doi.org/10.1016/S1474-4422(14)70156-5.
[3] Li MCH, Cook MJ. Deep brain stimulation for drug-resistant epilepsy. Epilepsia 2018;59(2):273–90. https://doi.org/10.1111/epi.13964.
[4] Satya-Murti S, Shepard KM, Helmers SL. Vagus nerve stimulation in the treatment of epilepsy. Neurology Clinical Practice 2013;3(5):431–5. https://doi.org/10.1212/CPJ.0b013e3182a3931f.
[5] Ellrich J. Transcutaneous auricular vagus nerve stimulation. J Clin Neurophysiol 2019;36(6):437. https://doi.org/10.1097/WNP.0000000000000576.
[6] Toffa DH, Touma L, Meskine TE, Bouthillier A, Nguyen DK. Learnings from 30 years of reported efficacy and safety of vagus nerve stimulation (VNS) for epilepsy treatment: a critical review. Seizure - European Journal of Epilepsy 2020;83:104–23. https://doi.org/10.1016/j.seizure.2020.09.027.
[7] Panov F, Ganaha S, Haskell J, et al. Safety of responsive neurostimulation in pediatric patients with medically refractory epilepsy. J Neurosurg Pediatr 2020;26(5):525–32. https://doi.org/10.3171/2020.5.PEDS20118.
[8] Warren AEL, Dalic LJ, Thevathasan W, Roten A, Bulluss KJ, Archer J. Targeting the centromedian thalamic nucleus for deep brain stimulation. J Neurol Neurosurg Psychiatry 2020;91(4):339–49. https://doi.org/10.1136/jnnp-2019-322030.
[9] Vonck K, Sprengers M, Carrette E, et al. A decade of experience with deep brain stimulation for patients with refractory medial temporal lobe epilepsy. Int J Neural Syst 2013;23(1):1250034. https://doi.org/10.1142/S0129065712500347.
[10] Velasco AL, Velasco F, Velasco M, Jiménez F, Carrillo-Ruiz JD, Castro G. The role of neuromodulation of the hippocampus in the treatment of intractable complex partial seizures of the temporal lobe. Acta Neurochir Suppl 2007;97(Pt 2):329–32. https://doi.org/10.1007/978-3-211-33081-4_36.
[11] Salanova V, Witt T, Worth R, et al. Long-term efficacy and safety of thalamic stimulation for drug-resistant partial epilepsy. Neurology 2015;84(10):1017–25. https://doi.org/10.1212/WNL.0000000000001334.

[12] Fisher R, Salanova V, Witt T, et al. Electrical stimulation of the anterior nucleus of thalamus for treatment of refractory epilepsy. Epilepsia 2010;51(5):899–908. https://doi.org/10.1111/j.1528-1167.2010.02536.x.

[13] Velasco AL, Velasco F, Velasco M, Trejo D, Castro G, Carrillo-Ruiz JD. Electrical stimulation of the hippocampal epileptic foci for seizure control: a double-blind, long-term follow-up study. Epilepsia 2007;48(10):1895–903. https://doi.org/10.1111/j.1528-1167.2007.01181.x.

[14] McLachlan RS, Pigott S, Tellez-Zenteno JF, Wiebe S, Parrent A. Bilateral hippocampal stimulation for intractable temporal lobe epilepsy: impact on seizures and memory. Epilepsia 2010;51(2):304–7. https://doi.org/10.1111/j.1528-1167.2009.02332.x.

[15] Tyrand R, Seeck M, Spinelli L, et al. Effects of amygdala–hippocampal stimulation on interictal epileptic discharges. Epilepsy Res 2012;99(1):87–93. https://doi.org/10.1016/j.eplepsyres.2011.10.026.

[16] Cukiert A, Cukiert CM, Argentoni-Baldochi M, et al. Intraoperative neurophysiological responses in epileptic patients submitted to hippocampal and thalamic deep brain stimulation. Seizure 2011;20(10):748–53. https://doi.org/10.1016/j.seizure.2011.07.003.

[17] Skelton HM, Brandman DM, Bullinger K, Isbaine F, Gross RE. Distinct biomarkers of ANT stimulation and seizure freedom in an epilepsy patient with ambulatory hippocampal electrocorticography. Stereotact Funct Neurosurg 2023;101(6):349–58. https://doi.org/10.1159/000533680.

[18] Silva AB, Khambhati AN, Speidel BA, Chang EF, Rao VR. Effects of anterior thalamic nuclei stimulation on hippocampal activity: chronic recording in a patient with drug-resistant focal epilepsy. Epilepsy & Behavior Reports 2021;16:100467. https://doi.org/10.1016/j.ebr.2021.100467.

[19] Voges BR, Schmitt FC, Hamel W, et al. Deep brain stimulation of anterior nucleus thalami disrupts sleep in epilepsy patients. Epilepsia 2015;56(8):e99–103. https://doi.org/10.1111/epi.13045.

[20] Drane DL, Pedersen NP. Finding the sweet spot: Fine-Tuning DBS parameters to cure seizures while avoiding psychiatric complications. Epilepsy Curr 2019;19(3):174–6. https://doi.org/10.1177/1535759719845326.

[21] Järvenpää S, Peltola J, Rainesalo S, Leinonen E, Lehtimäki K, Järventausta K. Reversible psychiatric adverse effects related to deep brain stimulation of the anterior thalamus in patients with refractory epilepsy. Epilepsy Behav 2018;88:373–9. https://doi.org/10.1016/j.yebeh.2018.09.006.

[22] Schulz R, Gerloff C, Hummel FC. Non-invasive brain stimulation in neurological diseases. Neuropharmacology 2013;64:579–87. https://doi.org/10.1016/j.neuropharm.2012.05.016.

[23] Polanía R, Nitsche MA, Ruff CC. Studying and modifying brain function with non-invasive brain stimulation. Nat Neurosci 2018;21(2):174–87. https://doi.org/10.1038/s41593-017-0054-4.

[24] Vöröslakos M, Takeuchi Y, Brinyiczki K, et al. Direct effects of transcranial electric stimulation on brain circuits in rats and humans. Nat Commun 2018;9(1):483. https://doi.org/10.1038/s41467-018-02928-3.

[25] Grossman N, Bono D, Dedic N, et al. Noninvasive deep brain stimulation via temporally interfering electric fields. Cell 2017;169(6):1029–1041.e16. https://doi.org/10.1016/j.cell.2017.05.024.

[26] Wessel MJ, Beanato E, Popa T, et al. Noninvasive theta-burst stimulation of the human striatum enhances striatal activity and motor skill learning. Nat Neurosci 2023;26(11):2005–16. https://doi.org/10.1038/s41593-023-01457-7.

[27] Acerbo E, Jegou A, Luff C, et al. Focal non-invasive deep-brain stimulation with temporal interference for the suppression of epileptic biomarkers. Front Neurosci 2022;16:945221. https://doi.org/10.3389/fnins.2022.945221.

[28] Missey F, Rusina E, Acerbo E, et al. Orientation of temporal interference for non-invasive deep brain stimulation in epilepsy. Front Neurosci 2021;15:633988. https://doi.org/10.3389/fnins.2021.633988.

[29] Botzanowski B, Donahue MJ, Ejneby MS, et al. Noninvasive stimulation of peripheral nerves using temporally-interfering electrical fields. Adv Healthcare Mater 2022;11(17):e2200075. https://doi.org/10.1002/adhm.202200075.

[30] Carmona-Barrón VG, Fernández del Campo IS, Delgado-García JM, De la Fuente AJ, Lopez IP, Merchán MA. Comparing the effects of transcranial alternating current and temporal interference (tTIS) electric stimulation through whole-brain mapping of c-Fos immunoreactivity. Front Neuroanat 2023;17. https://doi.org/10.3389/fnana.2023.1128193.

[31] Song S, Zhang J, Tian Y, Wang L, Wei P. Temporal interference stimulation regulates eye movements and neural activity in the mice superior colliculus. Annu Int Conf IEEE Eng Med Biol Soc 2021;2021:6231–4. https://doi.org/10.1109/EMBC46164.2021.9629968.

[32] Missey F, Ejneby MS, Ngom I, et al. Obstructive sleep apnea improves with non-invasive hypoglossal nerve stimulation using temporal interference. Bioelectron Med 2023;9(1):18. https://doi.org/10.1186/s42234-023-00120-7.

[33] Botzanowski B, Acerbo E, Lehmann S, et al. Controlling focality and intensity of non-invasive deep brain stimulation using multipolar temporal interference in non-human primates and rodents. Published online September 6, 2023: 2023.09.05.556444. doi:10.1101/2023.09.05.556444.

[34] Violante IR, Alania K, Cassarà AM, et al. Non-invasive temporal interference electrical stimulation of the human hippocampus. Nat Neurosci 2023;26(11):1994–2004. https://doi.org/10.1038/s41593-023-01456-8.

[35] Medina Villalon S, Paz R, Roehri N, et al. EpiTools, A software suite for presurgical brain mapping in epilepsy: intracerebral EEG. J Neurosci Methods 2018;303:7–15. https://doi.org/10.1016/j.jneumeth.2018.03.018.

[36] IT'IS database for thermal and electromagnetic parameters of biological tissues – ScienceOpen. https://www.scienceopen.com/document?vid=a95fbaa4-efd8-429a-a59e-5e208fea2e45. [Accessed 15 April 2024].

[37] Colombet B, Woodman M, Badier JM, Bénar CG. AnyWave: a cross-platform and modular software for visualizing and processing electrophysiological signals. J Neurosci Methods 2015;242:118–26. https://doi.org/10.1016/j.jneumeth.2015.01.017.

[38] Roehri N, Pizzo F, Lagarde S, et al. High-frequency oscillations are not better biomarkers of epileptogenic tissues than spikes. Ann Neurol 2018;83(1):84–97. https://doi.org/10.1002/ana.25124.

[39] Cavarretta F, Carnevale NT, Tegolo D, Migliore M. Effects of low frequency electric fields on synaptic integration in hippocampal CA1 pyramidal neurons: implications for power line emissions. Front Cell Neurosci 2014;8:310. https://doi.org/10.3389/fncel.2014.00310.

[40] Migliore R, De Simone G, Leinekugel X, Migliore M. The possible consequences for cognitive functions of external electric fields at power line frequency on hippocampal CA1 pyramidal neurons. Eur J Neurosci 2017 Apr;45(8):1024–31. https://doi.org/10.1111/ejn.13325.

[41] Migliore M, Novara G, Tegolo D. Single neuron binding properties and the magical number 7. Hippocampus 2008;18:1122–30. https://doi.org/10.1002/hipo.20471.

[42] Hines ML, Carnevale NT. The NEURON simulation environment. Neural Comput 1997;9:1179–209. https://doi.org/10.1162/neco.1997.9.6.1179.

[43] Weiss SA, Orosz I, Salamon N, et al. Ripples on spikes show increased phase-amplitude coupling in mesial temporal lobe epilepsy seizure-onset zones. Epilepsia 2016;57(11):1916–30. https://doi.org/10.1111/epi.13572.

[44] Urrestarazu E, Chander R, Dubeau F, Gotman J. Interictal high-frequency oscillations (100-500 Hz) in the intracerebral EEG of epileptic patients. Brain 2007;130(9):2354–66. https://doi.org/10.1093/brain/awm149. Epub 2007 Jul 11. PMID:17626037.

[45] Mooij AH, Raijmann RCMA, Jansen FE, Braun KPJ, Zijlmans M. Physiological ripples (± 100 Hz) in spike-free scalp EEGs of children with and without epilepsy. Brain Topogr 2017;30(6):739–46. https://doi.org/10.1007/s10548-017-0590-y.

[46] Urrestarazu E, Chander R, Dubeau F, Gotman J. Interictal high-frequency oscillations (100–500 Hz) in the intracerebral EEG of epileptic patients. Brain 2007;130(9):2354–66. https://doi.org/10.1093/brain/awm149.

[47] Mina F, Benquet P, Pasnicu A, Biraben A, Wendling F. Modulation of epileptic activity by deep brain stimulation: a model-based study of frequency-dependent effects. Front Comput Neurosci 2013;7. https://doi.org/10.3389/fncom.2013.00094.

[48] Mirzakhalili E, Barra B, Capogrosso M, Lempka SF. Biophysics of temporal interference stimulation. Cell Syst 2020 Dec 16;11(6):557–572.e5. https://doi.org/10.1016/j.cels.2020.10.004.

[49] Gabriel C, Peyman A, Grant EH. Electrical conductivity of tissue at frequencies below 1 MHz. Phys Med Biol 2009;54(16):4863.

[50] Hill AV, Katz B, Solandt DY. Nerve excitation by alternating current. Proceedings of the Royal Society of London Series B - Biological Sciences 1997;121(821):74–133. https://doi.org/10.1098/rspb.1936.0053.

[51] Karimi F, Cassarà AM, Capstick M, Kuster N, Neufeld E. Safety of non-invasive brain stimulation in patients with implants: a computational risk assessment. J Neural Eng 2024;21(6):066005. https://doi.org/10.1088/1741-2552/ad8efa.

[52] Jacobs J, Golla T, Mader M, et al. Electrical stimulation for cortical mapping reduces the density of high frequency oscillations. Epilepsy Res 2014;108(10):1758–69. https://doi.org/10.1016/j.eplepsyres.2014.09.022.

[53] Paschen E, Elgueta C, Heining K, et al. Hippocampal low-frequency stimulation prevents seizure generation in a mouse model of mesial temporal lobe epilepsyHuguenard JR, Kadam SD, editors. eLife 2020;9:e54518. https://doi.org/10.7554/eLife.54518.

[54] Luff CE, Dzialecka P, Acerbo E, Williamson A, Grossman N. Pulse-width modulated temporal interference (PWM-TI) brain stimulation. Brain Stimul 2024;17(1):92–103. https://doi.org/10.1016/j.brs.2023.12.010.

[55] Acerbo E, Botzanowski B, Dellavale D, et al. Improved temporal and spatial focality of non-invasive deep-brain stimulation using multipolar single-pulse temporal interference with applications in epilepsy. Published online January 14, 2024: 2024.01.11.575301. doi:10.1101/2024.01.11.575301.

[56] Cukiert A, Cukiert CM, Burattini JA, Mariani PP, Bezerra DF. Seizure outcome after hippocampal deep brain stimulation in patients with refractory temporal lobe epilepsy: a prospective, controlled, randomized, double-blind study. Epilepsia 2017;58(10):1728–33. https://doi.org/10.1111/epi.13860.

[57] Cukiert A, Cukiert CM, Burattini JA, Mariani PP. Long-term seizure outcome during continuous bipolar hippocampal deep brain stimulation in patients with temporal lobe epilepsy with or without mesial temporal sclerosis: an observational, open-label study. Epilepsia 2021;62(1):190–7. https://doi.org/10.1111/epi.16776.

[58] Velasco F, Velasco M, Velasco AL, Menez D, Rocha L. Electrical stimulation for epilepsy: stimulation of hippocampal foci. Stereotact Funct Neurosurg 2001;77(1–4):223–7. https://doi.org/10.1159/000064610.

[59] Lamoš M, Bočková M, Missey F, et al. Noninvasive temporal interference stimulation of the subthalamic nucleus in Parkinson's Disease reduces beta activity. Mov Disord 2025;40(6):1051–60. https://doi.org/10.1002/mds.30134.

[60] Karakis I, Lynam C, Taraschenko O, Staikova E, Drane DL. Concurrent EEG monitoring helps interpret neuropsychological testing results in patients with epilepsy. Epilepsy Behav 2020;111:107275. https://doi.org/10.1016/j.yebeh.2020.107275.

[61] Glennon JM, Weiss-Croft L, Harrison S, Cross JH, Boyd SG, Baldeweg T. Interictal epileptiform discharges have an independent association with cognitive impairment in children with lesional epilepsy. Epilepsia 2016;57(9):1436–42. https://doi.org/10.1111/epi.13479.

[62] Dinkelacker V, Xin X, Baulac M, Samson S, Dupont S. Interictal epileptic discharge correlates with global and frontal cognitive dysfunction in temporal lobe epilepsy. Epilepsy Behav 2016;62:197–203. https://doi.org/10.1016/j.yebeh.2016.07.009.

[63] Drane DL, Ojemann JG, Kim MS, et al. Interictal epileptiform discharge effects on neuropsychological assessment and epilepsy surgical planning. Epilepsy Behav 2016;56:131–8. https://doi.org/10.1016/j.yebeh.2016.01.001.

[64] Simula S, Daoud M, Ruffini G, Biagi MC, Bénar CG, Benquet P, Wendling F, Bartolomei F. Transcranial current stimulation in epilepsy: a systematic review of the fundamental and clinical aspects. Front Neurosci 2022 Aug 25;16:909421. https://doi.org/10.3389/fnins.2022.909421. PMID: 36090277; PMCID: PMC9453675.

[65] Simula S, Makhalova J, Pizzo F, Garnier E, Damiani G, Mercadal B, Chiara Biagi M, Salvador R, Medina-Villalon S, Ruffini G, Wendling F, George Bénar C, Bartolomei F. Impact of transcranial electrical stimulation on simultaneous stereoelectroencephalography recordings: a randomized sham-controlled study. Clin Neurophysiol 2024 Oct;166:211–22. https://doi.org/10.1016/j.clinph.2024.08.003. Epub 2024 Aug 14. PMID: 39182340.

[66] Schaeffer EL, Haber I, Fan Z, Bruno S, Mat B, Alauddin T, Neumann L, Smith R, Missey F, Williamson A, Beerli S, Capstick M, Neufeld E, Kuster N, Goldman RI, Davidson RJ, Albantakis L, Jones SG, Cirelli C, … Tononi G. (s. d.). Enhancement of sleep slow wave activity using transcranial electrical stimulation with temporal interference. medRxiv preprint. doi: 10.1101/2025.08.11.25333452.